Supporting Information

Dissecting the Self-assembly Dynamics of Imperfect Repeats in α-Synuclein

Fengjuan Huang[1], Ying Wang[2], Yu Zhang[2], Chuang Wang[3], Jiangfang Lian[1,3]*, Feng Ding[4]*, Yunxiang Sun[2,4]*

1. Ningbo Institute of Innovation for Combined Medicine and Engineering (NIIME), Ningbo Medical Center Lihuili Hospital, Ningbo 315211, China
2. School of Physical Science and Technology, Ningbo University, Ningbo 315211, China
3. School of Medicine, Ningbo University, Ningbo 315211, China
4. Department of Physics and Astronomy, Clemson University, Clemson, SC 29634, United States

*E-mail: hjmpin@163.com, fding@clemson.edu, sunyunxiang@nbu.edu.cn

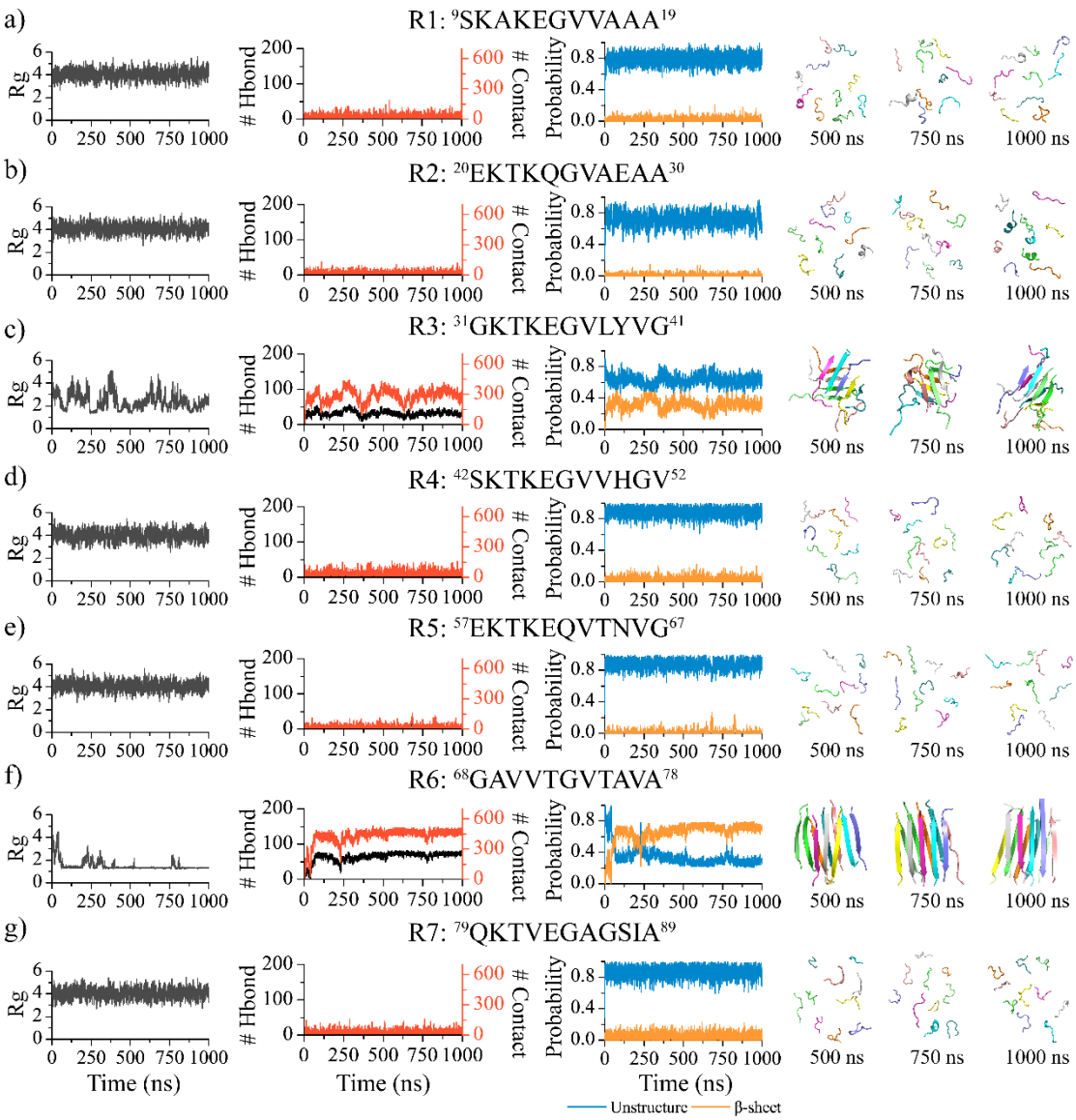

Figure S1. Equilibrium assessment for the simulation of each αS repeat. Time evolution of the radius of gyration (Rg (nm), first column), number of inter-peptide backbone hydrogen bonds and contacts (second column), as well as the probability of β-sheet and unstructured (random coil and bend, third column) formations for each repeat are used to illustrated that all the molecular system are well equilibrium **a-g)**. Snapshots at 500, 750, and 1000 ns from each representative trajectory are also presented. For each molecular system, one representative trajectory was randomly selected from thirty independent DMD simulations.

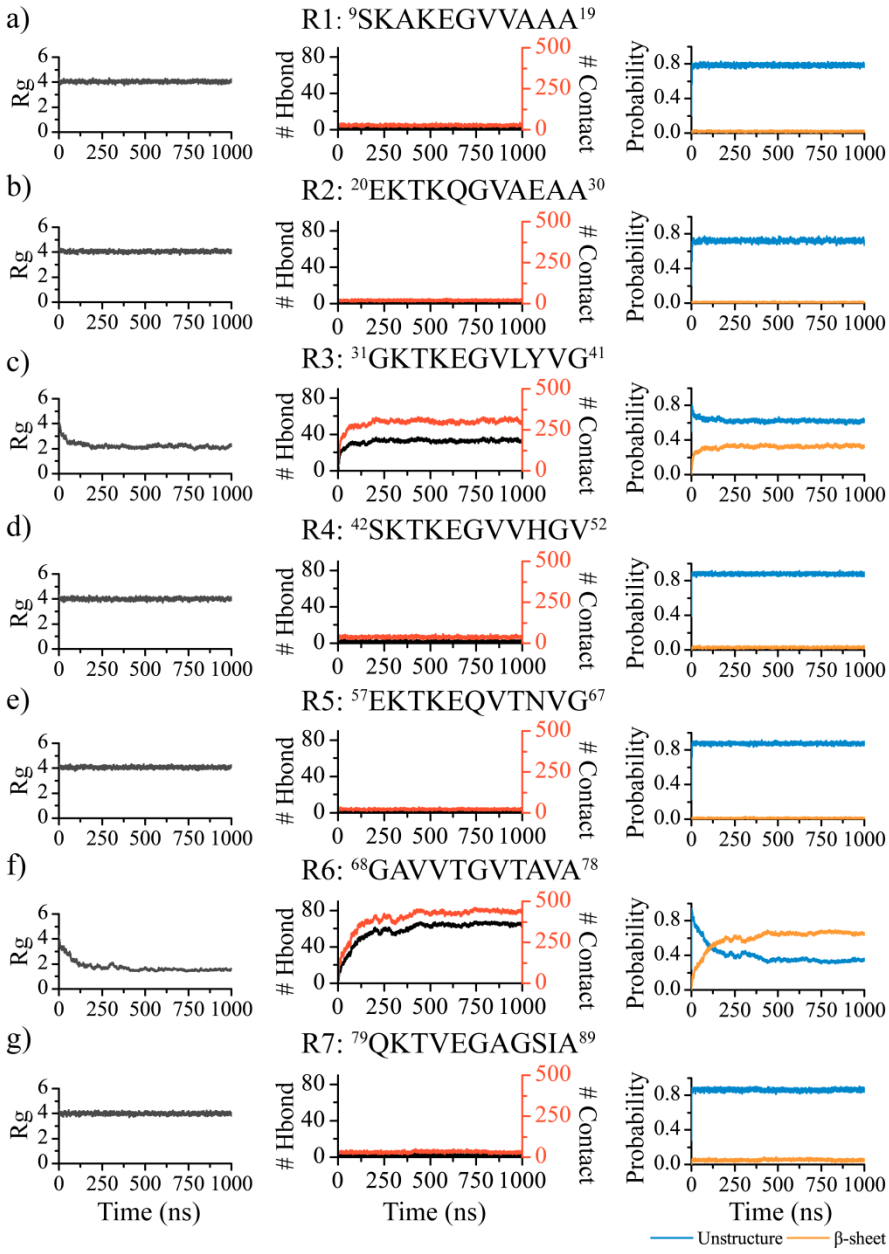

Figure S2. The ensemble-average convergence assessments for the simulations of each αS repeat. The time evolution of radius gyration (Rg (nm), first column), number of inter-peptide backbone hydrogen bonds and contacts (second column), and probability of β-sheet and unstructured formations (third column) averaged over all 30 independent DMD simulations of each αS repeat.

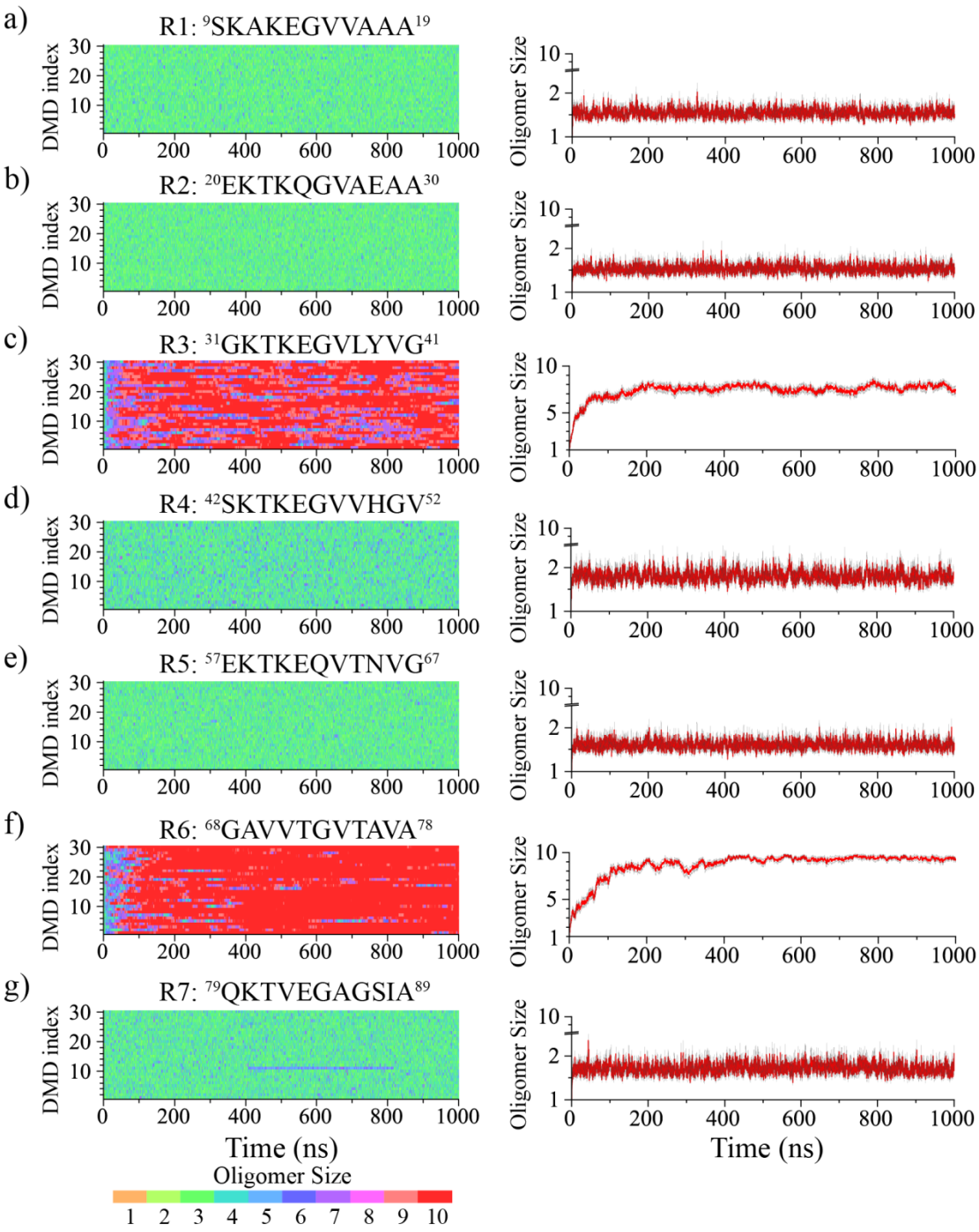

Figure S3. Sampling efficiency analysis for the DMD simulations of each αS repeat. The left panel shows the time evolution of the largest oligomer size in each independent DMD trajectory for each molecular system. The right panel shows the time evolution of the ensemble-average mass-weighted oligomer size using all thirty independent DMD trajectories, represented by the red line. The grey error bars represent the standard error of the mean from the ensemble average over all trajectories.

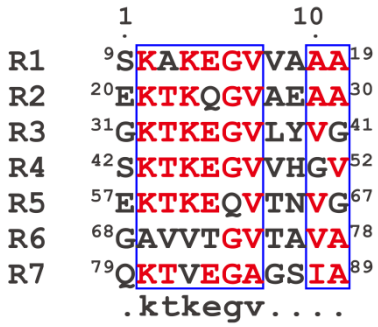

Figure S4. The sequence alignment of αS repeats. The highly conserved amino acids are highlighted in red. Residues with a consensus greater than 70% are illustrated in lowercase at the bottom.

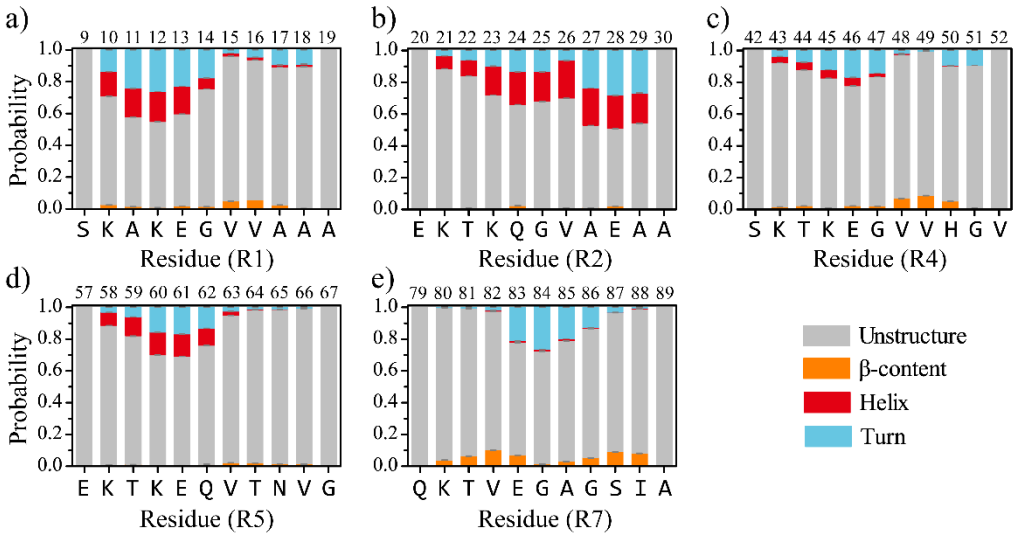

Figure S5. Secondary structure analysis for each residue in self-assemblies of R1, R2, R4, R5, and R7. The average propensity of each residue adopting unstructured, β-sheet, helix, and turn conformations within the self-assemblies of R1 **a)**, R2 **b)**, R4 **c)**, R5 **d)**, and R7 **e)** repeats is shown. The analysis is performed using the last 400 ns of 1000 ns trajectories from thirty independent DMD simulations.

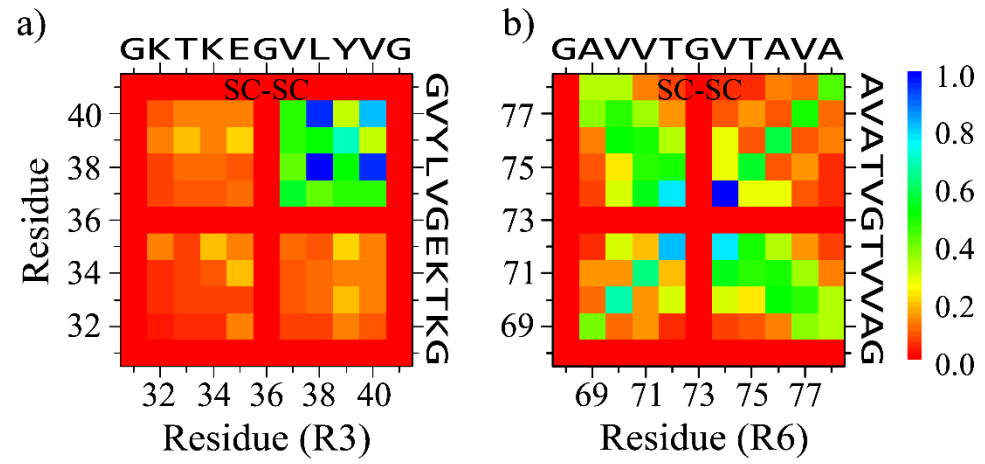

Figure S6. Residue-pairwise contact frequency analysis within the self-assemblies of R3 and R6 repeats. Side-chain residue-pairwise contact frequency analysis within the self-assemblies of R3 **a)** and R**6)** repeats.

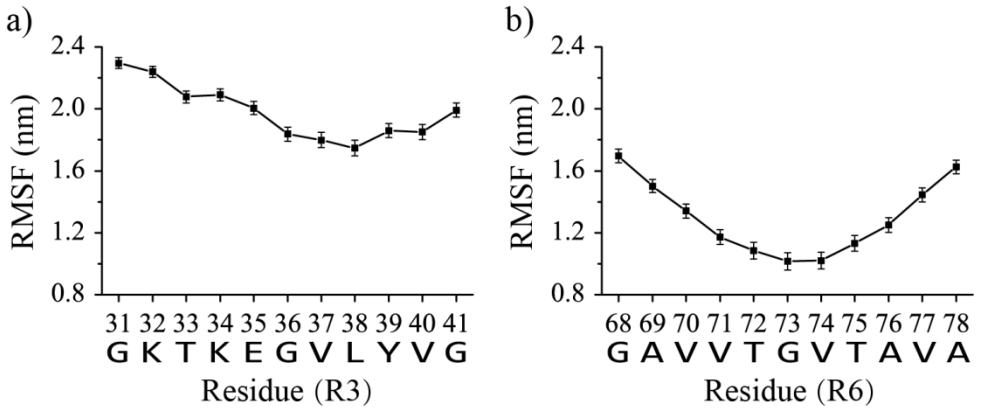

Figure S7. Root-mean-square fluctuation (RMSF) per residue within the self-assemblies of R3 and R6. The averaged RMSF per residue of R3 **a)** and R6 **b)** within their aggregates during the last 400 ns from 30 independent DMD trajectories is shown.